IOPscience iopscience.iop.org

Home Search Collections Journals About Contact us My IOPscience

Recent experimental advances in precision Casimir force measurements with the atomic force microscope

This article has been downloaded from IOPscience. Please scroll down to see the full text article.

2006 J. Phys. A: Math. Gen. 39 6233

(http://iopscience.iop.org/0305-4470/39/21/S14)

View the table of contents for this issue, or go to the journal homepage for more

Download details:
IP Address: 171.66.16.104
The article was downloaded on 03/06/2010 at 04:30

Please note that terms and conditions apply.

INSTITUTE OF PHYSICS PUBLISHING JOURNAL OF PHYSICS A: MATHEMATICAL AND GENERAL

J. Phys. A: Math. Gen. **39** (2006) 6233–6244 doi:10.1088/0305-4470/39/21/S14

Recent experimental advances in precision Casimir force measurements with the atomic force microscope

F Chen and U Mohideen

Department of Physics, University of California, Riverside, CA 92521, USA

E-mail: umar.mohideen@ucr.edu

Received 4 November 2005, in final form 8 January 2006
Published 10 May 2006
Online at stacks.iop.org/JPhysA/39/6233

Abstract

Advances in experimental methodology and analysis implemented in the precision measurement of the Casimir force with semiconductor surfaces are discussed. An experiment for the alteration of the Casimir force through a modification of the free carrier density in semiconductors is presented.

PACS numbers: 12.20.Fv, 12.20.Ds, 68.37.Ps

1. Introduction

The Casimir effect [1–6], in general, has recently gained a lot of prominence due to its importance in many subfields in fundamental and applied physics. As Casimir forces dominate material interactions at micron and submicron distance scales, precision experimental measurements of the Casimir force have become increasingly important. From a theoretical point of view, modern unification [7–13] theories require the presence of compactified extra spatial dimensions greater than three and this has motivated experimental searches for new forces at very short distance scales. From the point of technology, the remarkable development of micromachines with the modern nanofabrication techniques has added another urgent dimension to the study of Casimir forces. These microelectromechanical devices have moving parts separated by submicron distances, a region where the Casimir force between the interacting surfaces is very strong [14, 15].

Recently, we have explored the role of the Casimir force with semiconductor surfaces. We have performed a precise measurement of the Casimir force between a single crystal silicon plate and a gold-coated sphere using the AFM [16]. Here we discuss the improvements in the experiment and data analysis over our previous precision experiments of the Casimir force using the AFM [17–21]. Next, we also analyse an experiment for the modification of the Casimir force through a change of the dielectric properties of the boundary. The dielectric properties of semiconductors can be modified by changing the carrier density through an absorption of photons. Such an alteration of the dielectric properties will in

 © 2006 IOP Publishing Ltd Printed in the UK

turn modify the Casimir force between the semiconductor surface and the gold-coated sphere. The experimental details about the required parameters for the observation of the force are reviewed. These experiments are also important from a technological point of view, given that semiconductor materials such as silicon are central to the fabrication of micromachines.

Precision experimental measurement of the Casimir force has seen rapid developments in the last few years. Historically, the first experimental tests of the Casimir force were carried out by Sparnaay [22, 23] using a spring balance. A more unambiguous detection of the Casimir force was performed by Overbeek and von Blockland [24]. These early experiments realized that metallic or highly conductive boundaries are essential for controlling the systematic errors from residual electrostatic charges and work function differences [22–24]. We should note that an early attempt to measure the Casimir force in semiconductor surfaces and modify them with light was reported in [25]. Attractive forces were measured between a glass lens and a Si plate and also between the glass lens coated with a 2 mm diameter of amorphous Si and the Si plate. However, the glass lens is an insulator and therefore the electrical forces, such as, due to work function potential differences could not be controlled. This might also explain that no force change occurred on illumination for small separations below 350 nm [25] where it should have been most pronounced, given the approximate inverse third power distance dependence of the Casimir force for this geometry. A more detailed review of the historical experiments is given in [6].

More recently, the first modern experimental test of the Casimir force was performed by Lamoureaux [26] using the torsion balance. Subsequently, we have reported precision measurements of the Casimir force using the AFM [17–21]. In this paper, we will not review our earlier experiments with metallic surfaces. We will also not discuss our previous experiments demonstrating the lateral Casimir force using corrugated surfaces [27, 28], which was first theoretically predicted by Golestanian and Kardar [29]. Our present efforts in this direction involve experiments to check for nonlinearities in the lateral Casimir force resulting from diffraction-like effects from the use of the corrugated boundaries [30]. In terms of an overview we should note that an improved Casimir force measurement with parallel metal plates has recently been reported [31]. We should also note that the role of Casimir forces in microelectromechanical (MEM) machines, was directly demonstrated by Capasso *et al* [32, 33], where the Casimir force itself was used to actuate a MEMs device. In turn the MEMs device has been used in precise measurements of the Casimir force [34]. More developments in both these groups are presented elsewhere in this issue.

In section 2, a brief overview of the theoretical factors necessary for the calculation of the Casimir force is provided. In section 3, the precision experimental measurement of the normal Casimir force with the semiconductor test body is reported. In section 4, the experiment to modulate the Casimir force through an alteration of the carrier density in semiconductors is discussed. Section 5 is the conclusion.

2. Theoretical calculation of the normal Casimir force between a gold surface and silicon surface

To measure the Casimir force between two surfaces, the preference is to replace one of the plates by a metal sphere of radius R. The use of a large sphere instead of a plate avoids any problems associated with the parallel alignment of the two plates. If the boundaries of the large sphere and the plate have infinite conductivity (perfect or ideal metals), and their surfaces are separated by z, the Casimir force between them is [35] given by

$$F_{\mathrm{c}}^{0}(z) = \frac{-\pi^3}{360} R \frac{\hbar c}{z^3}. \tag{1}$$

In the above, the proximity force approximation [35–37] has been used to generalize the results of the Casimir force between two parallel plates to the case of the Casimir force between a large sphere and a plate. The errors introduced by the use of this approximation have been recognized to be much less than 1% [36]. In reality, one does not have access to perfect metals and the exact material properties of the boundaries used have to be taken into account [38, 39]. For two dissimilar materials such as the gold-coated sphere and silicon plate as used here, it is given by

$$F_{\rm c}(z) = \frac{R\hbar}{2\pi}\int_0^\infty k_\perp \,{\rm d}k_\perp \int_0^\infty {\rm d}\xi \left\{\ln\left[1 - r_\parallel^{(1)} r_\parallel^{(2)}\, {\rm e}^{-2qz}\right] + \ln\left[1 - r_\perp^{(1)} r_\perp^{(2)}\, {\rm e}^{-2qz}\right]\right\}. \tag{2}$$

The reflection coefficients for two independent polarizations are given by

$$r_\parallel^{(p)} = \frac{\varepsilon^{(p)}({\rm i}\xi)q - k^{(p)}}{\varepsilon^{(p)}({\rm i}\xi)q + k^{(p)}}, \qquad r_\perp^{(p)} = \frac{k^{(p)} - q}{k^{(p)} + q},$$

where $q^2 \equiv k_\perp^2 + \xi^2/c^2$, $k^{(p)^2} \equiv k_\perp^2 + \varepsilon^{(p)}({\rm i}\xi)\xi^2/c^2$ and $\varepsilon^{(p)}(\omega)$ is the dielectric permittivity of gold ($p = 1$) and silicon ($p = 2$). $\varepsilon^{(1)}({\rm i}\xi)$ was found by means of the dispersion relation from the imaginary part of $\varepsilon^{(1)}(\omega)$ obtained using the complex refractive index from tables [40]. The same procedure was used for single crystal Si. Since the optical properties of the Si at low frequencies depend on the concentration of charge carriers, the tabulated data in [40], obtained for a sample of high resistivity $\rho_0 = 1000\ \Omega$ cm, should be adapted for the silicon plate used in the experiment with a resistivity $\rho_0 = 0.0035\ \Omega$ cm. This is achieved [40] by adding the imaginary part of the Drude dielectric function to the imaginary part of the dielectric permittivity obtained using the data from tables. The plasma frequency at this resistivity was found to be 7×10^{14} rad s^{-1}, and relaxation parameter $\gamma = 1.5 \times 10^{14}$ s^{-1} [40]. It should be noted, that because of the small value of the plasma frequency compared to the characteristic frequency $c/2z$, where z is the separation distance, even a 50% change in the plasma frequency of Si leads to a less than 1% change in Casimir force magnitudes within the entire separation region presented here [16].

In addition to the corrections due to the dielectric properties, there are also corrections resulting from the roughness [16–21, 34, 41, 42]. The roughness of the surfaces used in the experiment stochastically alters the separation distance between the surfaces. The roughness correction can be made negligible by using smooth metal coatings. One of the advantages of using a single crystal silicon surface is that the roughness correction is drastically minimized when compared to the metal plate. In the experiments discussed here the roughness amplitude was decreased and the roughness contribution was made much less than 1% of the measured force even at the shortest separations. In earlier work [17–20], the roughness corrections were evaluated using a simple stochastic model for the surface roughness and the multiplicative approach was used to take into account the different corrections. In these experiments, we obtain more exact results for the contribution of surface roughness to the Casimir force using a nonmultiplicative approach. Diffraction and other correlation-type contributions [42] to the roughness correction were found to be negligible. Details on the application of the roughness correction are given in section 3.4.

In precision Casimir force measurements done at non-zero temperature, one has to also account for the role of thermal photons [43, 44]. At present, there are many different models for calculating the thermal correction to the Casimir force in the presence of real material boundaries [45–50]. However, in all the AFM-based experiments, the thermal corrections using any of the above models are much less than 1%. Thus, for the AFM-based experiments reported to date, the role of the thermal corrections can be neglected and the zero-temperature Casimir force as in equation (2) can be used.

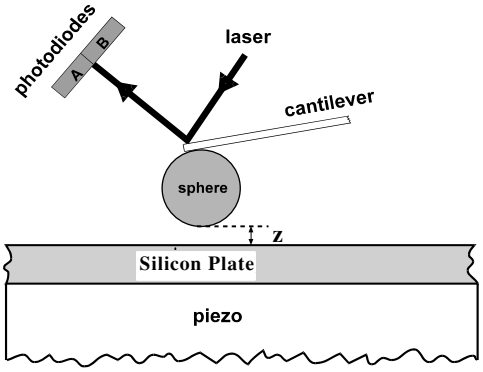

Figure 1. Schematic diagram of the experimental setup. Application of voltage to the piezo results in the movement of plate towards the sphere.

3. Experimental measurement of the normal Casimir force between a gold surface and silicon surface

We have adapted a contact mode AFM (shown in figure 1) to measure the Casimir force between a gold-coated sphere and single crystal silicon plate at pressures below 2×10^{-7} Torr. The force detection scheme in the AFM is based on a less than 1 μm thick cantilever beam. The ultra-thin cantilever beam flexes in response to a force on the sphere. A laser beam is reflected off the cantilever end to measure its deflection, leading to a difference signal between photodiodes A and B (shown in figure 4). This cantilever deflection signal is calibrated by electrostatic means and the procedure is described below. To prepare the cantilever, polystyrene spheres were mounted on the tip of 320 μm long cantilevers. The sphere is coated with 105 nm of gold. The diameter of the sphere was measured using a scanning electron microscope to be 202.6 ± 0.3 μm. A specially prepared single crystal silicon $\langle 1\,0\,0 \rangle$ is used as the plate. The resistivity data provided by the crystal grower were specified to be in the range (0.01–0.001) Ω cm. Using the four-probe technique we measured its precise resistivity to be $\rho = 0.0035$ Ω cm. As discussed in the introduction, the Si surface is strongly susceptible to oxidation, which will result in large electrostatic forces. This requires that the Si surface has to be carefully prepared to prevent the growth of the oxide. This was accomplished through a special passivation procedure. First nanostrip (a combination of H_2O_2 and H_2SO_4) is used to clean the surface of organics and other contaminants. This cleaning procedure oxidizes the surface. Next a 49% HF solution is used to etch the SiO_2. This procedure also leads to hydrogen termination of the surface silicon atoms [51, 52]. This hydrogen termination prevents the re-oxidation of the silicon surface as long as the silicon is kept in a high vacuum environment. The passivation is stable for more than 2 weeks under the 2×10^{-7} Torr pressure used in this experiment [51, 52]. In addition the vacuum system is oil free to prevent the presence of organic contaminants. We have checked the effectiveness of the passivation technique to prevent the contamination of the Si surface through the measurement of the distance dependence of the electrostatic force resulting from the residual potential difference between the interacting surfaces.

Care was taken to make ohmic electrical contacts to the silicon plate. Direct contact to the Si plate leads to large residual potentials. The electrical contact to the Si plate was made

from a 100 nm thick gold pad made on the silicon. The gold pad was made on the bottom of the Si plate.

In these experiments, a piezo capable of extending to a length greater than 6 μm was used. Such large piezo extensions were found necessary to allow time for the decay of noise associated with the separation of the gold sphere and plate after contact of the two surfaces. The complete movement of the piezo ($z_{\rm piezo}$) was calibrated using a fibre optic interferometer [53]. To extend and contract the piezo, continuous triangular voltages at 0.02 Hz are applied to the piezo. Given that the experiment is done at room temperature, applying of static voltages will lead to piezo creep and loss of position sensitivity. The extension and contraction of the piezo were fit to terms up to fourth order in the applied voltage.

3.1. Calibration, measurement of the residual electrostatic force and the deflection coefficient

The general experimental technique is similar to what we have used in our previous work. Many improvements have been applied to this technique in our recent measurements. All calibration and other measurements are done at the same time as the Casimir force measurement in the same high vacuum apparatus. The calibration of the deflection signal of the cantilever ($S_{\rm def}$) and the residual potential difference between the gold-coated sphere and silicon plate is done by measuring the distance dependence of an applied electrostatic force. In addition, a small correction has to be applied to the separation distance between the gold sphere and the Si plate due to the movement of the cantilever. The actual separation distance z between the bottom of the gold sphere and the Si plate is given by

$$z = z_{\rm piezo} + S_{\rm def} m + z_0. \tag{3}$$

Here, $z_{\rm piezo}$ is the distance moved by the piezo, $S_{\rm def}$ is the cantilever deflection signal from the photodiodes (it has negative values for attractive forces), m is the deflection coefficient in units of nm per unit deflection signal and z_0 is the average separation on contact of the gold surface and the Si plate. It is non-zero due to the stochastic roughness of the surfaces and its determination is described in a later section. The deflection coefficient m can also be measured by the application of electrostatic forces between the gold sphere and Si plate [20].

In our measurements here, the gold sphere was kept grounded. The electrical contact to the gold sphere was accomplished by applying a very thin gold coating to the cantilever. The electrostatic force between the gold sphere and the silicon plate is given by [54]

$$F_{\rm elec} = 2\pi\varepsilon_0 (V_1 - V_0)^2 \sum_{n=1}^{\infty} {\rm csch}\, n\alpha ({\rm coth}\ \alpha - n\ {\rm coth}\ n\alpha). \tag{4}$$

Here 'V_1' is the voltage applied to the silicon plate and 'V_0' is the residual potential difference between the grounded gold sphere and silicon plate. The quantity $\alpha = \cosh^{-1}\left(1 + \frac{z}{R}\right)$, where R is the radius of the sphere, z is distance between the surfaces. As equation (4) is cumbersome to perform fitting of experimental data to the theory, in our recent experiments, a perturbative version of equation (4) is used, where the electrostatic force is given by

$$F_{\rm elec} = -2\pi\varepsilon_0 (V_1 - V_0)^2 \sum_{m=0}^{7} A_m t^{m-1}, \tag{5}$$

where $t = \left(\frac{z}{R}\right)$ and the coefficients A_0 through A_7 are given by 0.5, −1.182 60, 22.2375, −571.366, 9592.45, −90 200.5, 38 3084, −30 0357 respectively. This expansion when compared to the complete equation (4) has a relative error of 4.7×10^{-5} and 1.5×10^{-5} at separation distances of 1.5 μm and 5.0 μm respectively.

First, different dc voltages between +0.2 and −0.4 V are applied to the plate. The cantilever deflection signal is measured as a function of the distance. The 0.02 Hz triangular

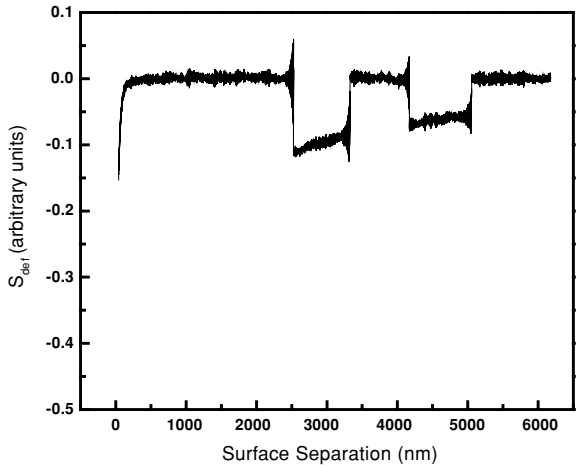

Figure 2. The deflection signal of the cantilever in response to the dc voltage and two square voltage pulses applied to the Si plate as a function of distance. This improved calibration method avoids the need for background subtraction.

wave was applied to the piezo to change the distance between the sphere and the plate. This electric force measurement at each voltage was repeated five times and the average electric force curve was used. Larger applied voltages will lead to more cantilever deflection and therefore earlier contact of the two surfaces. The change in the contact position of the sphere and the plate as a function of the applied voltage can then be used to measure deflection coefficient m [20]. In order to determine the contact of the two surfaces precisely, 32 768 data points at equal time intervals were acquired for each force measurement. In cases, where the contact point was between two neighbouring data points a linear interpolation was used to identify the exact value. The deflection coefficient was found to be $m = 43.3 \pm 0.3$ nm per unit deflection signal. This value of m as shown in equation (3) was used to correct the separation distance in all measurements.

For the calibration of the deflection signal and the determination of the residual potential between the two surfaces, an improved method, rather than a simple application of a dc voltage to the plate was used here. This was done to avoid systematic errors due to scattered laser light. In addition to the application of the dc voltage to the Si plate described previously, a square voltage pulse of amplitude +0.4 V and time interval corresponding to a separation distance between 1 and 5 μm was also applied to the plate. Figure 2 shows the deflection signal of the cantilever in response to both the applied dc voltage and the square pulse as a function of the separation distance between the gold sphere and Si plate. By measuring only the difference in signal during the pulse allows one to avoid the need for a background subtraction. Also the large width of the pulse allowed checks for the distance dependence of the residual potential and any position dependence in the calibration. Equation (5) is used to fit the difference signal and the residual potential difference was measured to be $V_0 = -0.114 \pm 0.002$ V. The calibration of the cantilever deflection signal was also done by fitting the difference signal on application of the voltage pulse to equation (5). Note that for the high conductivity Si plate used, the width of the space charge region is negligible for the voltages and separation distances considered here. The signal calibration constant was determined to be 1.440 ± 0.007 nN per unit cantilever deflection signal.

3.2. Experimental measurement of the Casimir force

Next the experimental measurement of the Casimir force between the sphere and the plate as a function of the separation distance is performed. The gold sphere is kept grounded while a compensating voltage corresponding to V_0 is applied to the plate to cancel the residual electrostatic force. The distance between the plate and the sphere is varied again by applying continuous triangular voltages at 0.02 Hz to the piezo. The force data $F^{\rm expt}(z)$ were collected at 32 768 equal time intervals as the distance between the sphere and plate was changed. This measurement was repeated 65 times. Even with such closely spaced data points special precautions have to be observed during the averaging of the 65 measurements.

A great advantage of the AFM technique in the averaging is that the contact point between the two surfaces z_0 provides a starting point for alignment of all the 65 measurements. Nevertheless, thermal noise in cantilever deflection signal, $S_{\rm def}$, leads to noise in the corresponding separations z because of the deflection correction applied in equation (3). To account for this in the averaging, the separation distance is divided into a grid of 32 768 equidistant points separated by 0.17 nm. For each measured Casimir force–distance curve, the value of the force at the grid point is computed using linear interpolation of the neighbouring two data points. Because the separation distance between neighbouring points is as small as 0.17 nm, higher order interpolation procedures were not required. This was confirmed by a statistical check of the data as described in another paper in this proceedings issue. Also the noise spectrum and amplitude of the interpolated data were confirmed to be the same as the raw data. This allowed the averaging of the 65 Casimir force measurements even including the effect of the change in the separation distance due to the thermal noise of cantilever. Data for separations below 62.33 nm up to contact are not presented as nonlinearities associated with the 'jump to contact' introduce uncontrollable errors into the force measurement.

3.3. Determination of the separation distance on contact

The separation distance on contact of the two surfaces z_0 needs to be independently determined for a comparison of the measured Casimir force to the theory. The electrostatic force curves measured with the application of dc voltages used in the determination of the deflection coefficient m were used to determine z_0. In difference from our earlier work, here we attempted to reduce the role of uncertainties in the determination of V_0 in the determination of z_0. This procedure also allows an independent check of the distance dependence of V_0 (this is important given the semiconductor surfaces are susceptible to accumulation of charges and defects). To accomplish this, the electrostatic force between the sphere and plate shown in equation (5) is rewritten as

$$F_{\rm elec} = C_{\rm elect}(z)(V_1 - V_0)^2 \tag{6}$$

and

$$C_{\rm elec} = -2\pi\varepsilon_0 \sum_{m=0}^{7} A_m t^{m-1}. \tag{7}$$

The parabolic dependence of the electric force on the applied voltage V_1 and the residual potential V_0 can be used to make a second independent determination of V_0 [24, 55]. The signal deflection is first measured for many dc voltages applied to the Si plate as described previously in section 3.1. The experimentally measured average Casimir force deflection signal (before conversion to force) measured in the last section is subtracted from the total to yield only the signal due to the electrostatic force. For a given distance z, the electric force is plotted as a function of applied voltage V_1 to the plate. The resulting parabolas are fit to

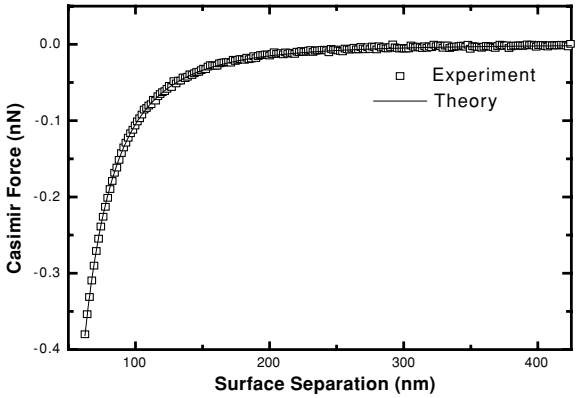

Figure 3. The average measured Casimir force (open squares) is plotted as a function of the separation distance. The solid line represents the theory.

provide a value for the V_0 and $C_{\rm elec}(z)$. This is repeated for many different z. The V_0 was found to be same as that determined earlier and to be independent of separation distance. Note that this measurement is also independent of errors in the cantilever calibration. In order to determine z_0, the $C_{\rm elec}(z)$ are then plotted as a function of z and fit to equation (7). The value of z_0 so determined was 32.1 ± 0.8 nm. The uncertainty in z_0 includes the error in the deflection coefficient m and the calibration. It should be noted that this uncertainty is at the contact position and is not the uncertainty between data points. With this average separation distance on contact z_0, the separation distances between the gold sphere and silicon plate are completely determined. Note that this value of z_0 can be used iteratively to reduce the uncertainty in the calibration of the cantilever deflection.

3.4. Comparison of the experimental Casimir force to theory

At this point all the experimental parameters are determined and a comparison of the experiment to the theory can be attempted. The measured Casimir force between the gold sphere and the silicon plate in the distance range from 62.33 to 425 nm is shown as open squares in figure 3. For the purpose of clarity only every tenth data point is displayed in the figure.

For a comparison of the theoretical results with the experiment, we should take into account the surface roughness corrections. In order to do this the topography of the gold coating on the sphere and the silicon plate was measured using the AFM. The roughness was found to be stochastically distributed distortions with typical heights of 11–20 nm on the sphere and 0.3–0.6 nm on the silicon plate. There are also rare point-like peaks on the sphere with heights up to 25 nm. If v_k^p represents the fraction of the surface area with roughness height h_k^p ($p = 1$ for the gold sphere and $p = 2$ for the plate), one can find the zero roughness levels $H_0^1 = 15.35$ nm and $H_0^2 = 0.545$ nm. Using the additive approach, the theoretical Casimir force, including both finite conductivity and surface roughness corrections, can be calculated as [21]

$$F^{\rm theor}(z) = \sum_{k,j} v_k^1 v_j^2 F_{\rm c}(\bar{z}), \tag{8}$$

where $\bar{z} = z + H_0^1 + H_0^2 - h_k^1 - h_j^2$ and $F_{\rm c}(z)$ is given by equation (2). The theoretical Casimir force is shown as a solid line in figure 3.

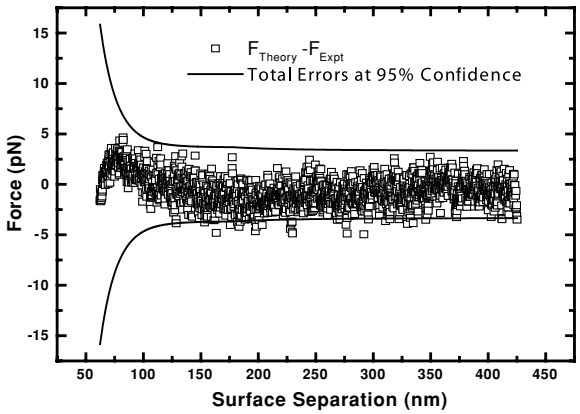

Figure 4. The solid line represents the error bars at 95% confidence level and the open squares represent the difference force between the experimental data point and the theory. The error bars are overestimated as much less than 5% of the data fall outside the error bars.

The statistical error analysis in the experiment and theory is discussed in detail in an accompanying article in this issue. The random errors in the experiment can be determined using the Student's t distribution tables with the number of degrees of freedom $f = n-1 = 64$ and choosing the 95% confidence level. The random noise in the experimental data represented by the variance is 1.5 pN. For a 95% confidence level this leads to a random error of 3.0 pN. The systematic errors in the experiment are due to the force calibration, instrumental sensitivity, computer resolution and instrumental resolution and lead to a total of 1.17 pN at the 95% confidence level. The theoretical force curves include errors due to use of proximity force theorem, and sample to sample variations in the optical data. Additional errors in the determination of the theory come from the uncertainty in the determination of the sphere radius and the separation distance on contact of the sphere and plate. In figure 4, the open squares represent the difference between the experimental data point and the theoretical force as a function of distance. The solid lines represent the total errors as a function of distance at the 95% confidence level. It can be seen that the error bars are slightly overestimated as much less than required 5% of the data points fall outside the error bars. If one takes the ratio of the error bars to the theoretical force value as a measure of the precision, then it is 3.8% within the separation region between 75.8 and 81.5 nm. It should be noted, however, that the actual difference between the theoretical and experimental force values is less than 1% of the force magnitude between separations of 62.33 to 69.98 nm.

4. Modulation of the Casimir force with plate conductivity

Here we discuss our experimental proposal to demonstrate the modulation of the Casimir force through a change in the conductivity. As can be realized from a study of equation (2), a change in the conductivity of the boundaries will lead to the modification of the Casimir force. The simplest method of altering the conductivity is by changing the free carrier density of the semiconductor boundary. This can be accomplished in two ways, either through a change in the temperature or by the excitation of free carriers through the absorption of photons. While changing the temperature to modify the boundary conductivity is a good method in theory, the temperature modification leads to large systematic errors in the measurement setup [56].

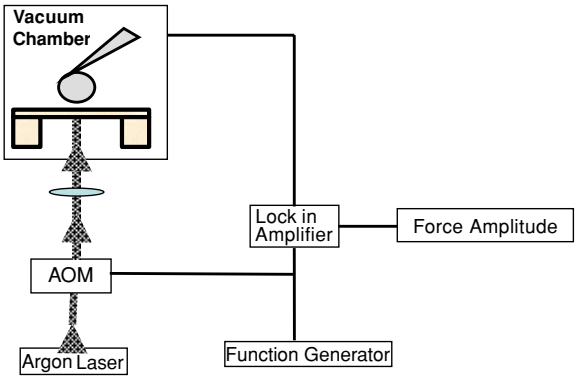

Figure 5. Experimental setup used for the modulation of the Casimir force through excitation of carriers in the semiconductor membrane shown.

The excited free carrier density has to be modified by greater than 10^{18} cm^{-3} in order to result in a fraction of a per cent change in the Casimir force for separation distances of order 100 nm. To accomplish such large changes in the free carrier density, specially designed silicon plates are needed. The effective volume of the silicon has to be kept very small to achieve the large free carrier densities. Thus fabrication of special silicon membranes is necessary. For carrier excitation, at equilibrium, the amount of optical power (P) required is given by:

$$P = \frac{\hbar\omega N}{\tau}, \tag{9}$$

where ω is the frequency of the light, N is the number of excited electrons and τ is the excited carrier lifetime. Si is an ideal material as its excited carrier lifetime is rather long around $\tau = 1$ ms (due to its indirect bandgap). However, this lifetime can be achieved only far from surfaces or other boundaries particularly those not containing impurities. In the case of passivated silicon membranes, carrier lifetimes of order $\tau > 10^{-6}$ s are achievable [57]. For membranes of 2 μm thickness, and a 514 nm laser light beam focused on a 100 μm diameter spot, modest light powers of 6 mW can lead to excited carrier densities of 10^{18} cm^{-3}.

The illumination of the silicon has to be done such that very little if any of the light impinges on the sphere, as this would lead to light-induced forces on the sphere. If the silicon is illuminated from the bottom, care should be taken that the fraction of light transmitted through the membrane leads to negligible amount of photon pressure on the sphere. Thus the thickness of the membrane has to be greater than the 1 μm optical absorption depth of silicon. Fabrication of a few micron thick silicon membrane is necessary to accomplish the necessary experimental conditions for the observation of the modulation of the Casimir force.

The experimental setup to be used for the measurement of the carrier-induced modulation of the Casimir force is shown in figure 5. The passivated silicon substrate containing the silicon membrane is replaced with the silicon plate shown in figure 1.

The same oil-free vacuum with a pressure of around 2×10^{-7} Torr is used. 10 mW of 514 nm light from an Argon laser will be focused on a 100 μm diameter spot on the bottom surface of the membrane. The light will be modulated at a frequency of 100 Hz (5 ms wide light pulses) using an acousto-optic modulator (AOM). The AOM is triggered with a function generator which is used as a reference for the lockin amplifier. The lockin amplifier measures the amplitude of the modulation of the Casimir force in response to the carriers excited by the light pulse. The calibration of the cantilever and the measurement of the residual potential

differences will be performed in a manner similar to that discussed in sections 3.1 and 3.2. A dc voltage of V_0 will be applied to the silicon membrane to compensate for the contact potential differences. With the excitation of the carriers however, the contact potential is modified. Thus additional voltage compensation V_0' is necessary in the presence of the excited carriers. So an additional square voltage pulse should be applied synchronous with the laser pulse. The amplitude of modulation of the Casimir force will be measured by the lockin amplifier.

5. Conclusions

Our recent precision measurements of the Casimir force have concerned interactions between semiconductor and metal surfaces. A precision Casimir force measurement between a gold sphere and Si plate was discussed in detail. Many improved experimental and analysis techniques were implemented such as higher vacuum, oil-free vacuum, single crystal Si plate, more precise measurement of the separation distance, improved calibration and measurement of residual potential differences and a rigorous statistical analysis of the data. In the present analysis at the 95% confidence level, the smallest ratio of the error bar to the force is 3.8% in the separation distance range between 75.8 and 81.5 nm. It should also be noted that the actual difference between the theoretical and experimental force values is less than 1% of the force magnitude within the separation region from 62.33 to 69.98. An experiment to measure the modulation of the Casimir force by exciting carriers in the silicon membrane was also presented.

Acknowledgments

This work was supported by NSF grant no. PHY0355092 and DOE grant no. DE-FG02-04ER46131. The authors acknowledge extensive help from G L Klimchitskaya and V M Mostepanenko for the theoretical analysis. The authors also acknowledge helpful discussions with R Decca, R Onofrio, D Iannuzzi, S Reynaud, A Lambrecht, K A Milton, I Brevik and B Sernelius.

References

[1] Casimir H B G 1948 *Proc. K. Ned. Akad. Wet.* **51** 793–5
[2] Milonni P W 1994 *The Quantum Vacuum: An Introduction to Quantum Electrodynamics* (New York: Academic)
[3] Mostepanenko V M and Trunov N N 1997 *The Casimir Effect and Its Applications* (Oxford: Clarendon)
[4] Schwinger J, DeRaad L L and Milton K A 1978 *Ann. Phys.* **115** 1–23
[5] Milton K A 2001 *The Casimir Effect* (Singapore: World Scientific)
[6] Bordag M, Mohideen U and Mostepanenko V M 2001 *Phys. Rep.* **303** 1–205
[7] Arkani-Hamed N, Dimopoulos S and Dvali G 1998 *Phys. Lett.* B **429** 263
[8] Randall L and Sundrum R 1999 *Phys. Rev. Lett.* **83** 3370
[9] Fischbach E and Talmadge C L 1999 *The Search for Non-Newtonian Gravity* (New York: Springer)
[10] Long J C, Chan H W, Churnside A B, Gulbis E A, Varney M C M and Price J C 2003 *Nature* **421** 922–5
[11] Hoyle C D, Kapner D J, Heckel B R, Adelberger E G, Gundlach J H, Schmidt U and Swanson H E 2004 *Phys. Rev.* D **70** 042004
[12] Bordag M, Geyer B, Klimchitskaya G L and Mostepanenko V M 1999 *Phys. Rev.* D **60** 055004
[13] Bordag M, Geyer B, Klimchitskaya G L and Mostepanenko V M 2000 *Phys. Rev.* D **62** 011701
[14] Serry F, Walliser D and Maclay G J 1998 *J. Appl. Phys.* **84** 2501–6
[15] Buks E and Roukes M L 2001 *Phys. Rev.* B **63** 033402
[16] Chen F, Mohideen U, Klimchitskaya G L and Mostepanenko V M 2005 *Phys. Rev.* A **72** 0201001
[17] Mohideen U and Roy A 1998 *Phys. Rev. Lett.* **81** 4549–52

[18] Klimchitskaya G L, Roy A, Mohideen U and Mostepanenko V M 1999 *Phys. Rev.* A **60** 3487–95
[19] Roy A, Lin C Y and Mohideen U 1999 *Phys. Rev.* D **60** (R)111101
[20] Harris B W, Chen F and Mohideen U 2000 *Phys. Rev.* A **62** 052109
[21] Chen F, Klimchitskaya G L, Mohideen U and Mostepanenko V M 2004 *Phys. Rev.* A **69** 022117
[22] Sparnaay M J 1958 *Physica* **24** 751–64
[23] Sparnaay M J 1989 *Physics in The Making* ed Sarlemijn ed A and Sparnaay M J (Amsterdam: North-Holland)
[24] Blokland P H G M V and Overbeek J T G 1978 *J. Chem. Soc. Faraday Trans.* **74** 2637–51
[25] Arnold W, Hunklinger S and Dransfeld K 1979 *Phys. Rev.* B **19** 6049
[26] Lamoreaux S K 1997 *Phys. Rev. Lett.* **78** 5–8
Lamoreaux S K 1998 *Phys. Rev. Lett.* **81** 5475 (erratum)
[27] Chen F, Mohideen U, Klimchitskaya G L and Mostepanenko V M 2002 *Phys. Rev. Lett.* **88** 101801-1-4
[28] Chen F, Mohideen U, Klimchitskaya G L and Mostepanenko V M 2002 *Phys. Rev.* A **66** 032113
[29] Golestanian R and Kardar M 1997 *Phys. Rev. Lett.* **78** 3421–4
[30] Buscher R and Emig T 2004 *Phys. Rev.* A **69** 062101
[31] Bressi G, Carugno G, Onofrio R and Ruoso G 2002 *Phys. Rev. Lett.* **88** 041804
[32] Chan H B, Aksyuk V A, Kleiman R N, Bishop D J and Capasso F 2001 *Science* **291** 1941–3
[33] Chan H B, Aksyuk V A, Kleiman R N, Bishop D J and Capasso F 2001 *Phys. Rev. Lett.* **87** 211801-1-4
[34] Decca R S, Fischbach E, Klimchitskaya G L, Krause D E, Lopez D and Mostepanenko V M 2003 *Phys. Rev.* D **68** 116003
[35] Derjaguin B V, Abrikosova I I and Lifshitz E M 1956 *Q. Rev.* **10** 295
[36] Schroder O, Scardicchio A and Jaffe R L 2005 *Phys. Rev.* A **72** 012105
[37] Blocki J, Randrup J, Swiatechi W J and Tsang C F 1977 *Ann. Phys.* **105** 427–62
[38] Lifshitz E M 1956 *Sov. Phys.—JETP* **2** 73–83
[39] Dzyaloshinskii I E, Lifshitz E M and Pitaevskii L P 1961 *Adv. Phys.* **10** 165–209
[40] Handbook of Optical Constants of Solids 1985 ed L P Pitaevskii (New York: Academic)
[41] Van Bree J L M J, Poulis J A, Verhaar B J and Schram K 1974 *Physica* **78** 187–90
[42] Genet C, Lambrecht A, Neto P M and Reynaud S 2003 *Europhys. Lett.* **62** 484–90
[43] Mehra J 1967 *Physica* **37** 145–52
[44] Brown L S and Maclay G J 1969 *Phys. Rev.* **184** 1272–9
[45] Genet G, Lambrecht A and Reynaud S 2000 *Phys. Rev.* A **62** 012110
[46] Bordag M, Geyer B, Klimchitskaya G L and Mostepanenko V M 2000 *Phys. Rev. Lett.* **85** 503–6
[47] Bostrom M and Sernelius B E 2000 *Phys. Rev. Lett.* **84** 4757–60
[48] Brevik I, Aarseth J B, Hoye J S and Milton K A 2005 *Phys. Rev.* **71** 056101
[49] Svetovoy V B and Lokhanin M V 2003 *Phys. Rev.* A **67** 022113
[50] Geyer B, Klimchitskaya G L and Mostepanenko V M 2003 *Phys. Rev.* A **67** 062102
[51] Graf D, Grundner M, Schulz R and Muhlhoff L 1990 *J. Appl. Phys.* **68** 5155–61
[52] Arima K, Endo K, Kataoka T, Oshikane Y, Inoue H and Mori Y 2000 *Appl. Phys. Lett.* **76** 463–5
[53] Chen F and Mohideen U 2001 *Rev. Sci. Instrum.* **72** 3100–02
[54] Smythe W R 1950 *Electrostatics and Electrodynamics* (New York: McGraw-Hill)
[55] Iannuzzi D, LIsanti M and Capasso F 2004 *Proc. Natl. Acad. Sci.* **101** 4019
[56] Chen F, Mohideen U and Milonni P W 2003 *Proc. 6th Workshop on Quantum Field Theory Under the Influence of External Conditions* ed Milton ed K A (Princeton, NJ: Rinton)
[57] Khanna V K 2004 *Eur. J. Phys.* **25** 221